



HAL
open science

Impacts of organic matter digestion protocols on synthetic, artificial and natural raw fibers

Robin Treilles, Aurélie Cayla, Johnny Gasperi, Bénédicte Strich, Patrick Ausset, Bruno Tassin

► To cite this version:

Robin Treilles, Aurélie Cayla, Johnny Gasperi, Bénédicte Strich, Patrick Ausset, et al.. Impacts of organic matter digestion protocols on synthetic, artificial and natural raw fibers. *Science of the Total Environment*, 2020, 748, p. 141230. 10.1016/j.scitotenv.2020.141230 . hal-02908818

HAL Id: hal-02908818

<https://hal.science/hal-02908818>

Submitted on 22 Aug 2022

HAL is a multi-disciplinary open access archive for the deposit and dissemination of scientific research documents, whether they are published or not. The documents may come from teaching and research institutions in France or abroad, or from public or private research centers.

L'archive ouverte pluridisciplinaire **HAL**, est destinée au dépôt et à la diffusion de documents scientifiques de niveau recherche, publiés ou non, émanant des établissements d'enseignement et de recherche français ou étrangers, des laboratoires publics ou privés.



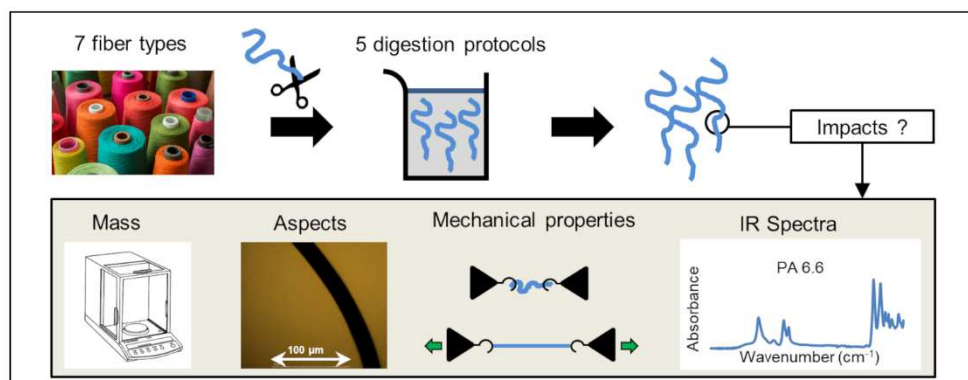
Distributed under a Creative Commons Attribution - NonCommercial 4.0 International License

1 Abstract

2 As microplastic (MPs) studies grow, environmental concerns of all kinds of fibers are currently
3 investigated. However, there is a gap in data regarding the impacts of digestion protocols on fibers
4 integrity. This work focuses on the impact of five commonly used digestion protocols on the seven
5 most produced fibers in traditional textile: three synthetics (polyamide 6.6 (PA 6.6), polyethylene
6 terephthalate (PET) and polyacrylonitrile (acrylic)), one artificial (viscose), two vegetal natural
7 (cotton and flax) and one animal natural (wool). The protocols to be tested were selected based on the
8 literature: 10 % KOH at 40 °C for 24 h; 10 % KOH at 60 °C for 24 h; diluted NaClO at room
9 temperature (~ 20 °C) for 15 h; 30 % H₂O₂ at 40 °C for 48 h; Fenton's reagent with 30% H₂O₂ for 2 h
10 at room temperature (~20 °C). The fibers were characterized before and after digestion. The effects of
11 those protocols on fibers integrity have been assessed using several of their performance parameters.
12 High degradations were observed for PET with 10 % KOH 60 °C whereas almost no impact was
13 observed at 40 °C. H₂O₂ digestion affects mechanical properties of different fibers, particularly
14 PA 6.6. Both protocols should be avoided for synthetic fibers analyses. NaClO digestion mainly
15 affected flax and viscose. Diluted NaClO at room temperature for 15 h, 10 % KOH at 40 °C for 24 h
16 and Fenton's reagent are more appropriate to maintain fibers integrity.

17 KEYWORDS: fibers, digestion protocols, impact assessment, microplastic

18 Graphical abstract



19

20 1. Introduction

21 Recent research on plastic pollution has raised environmental concerns about synthetic fibers
22 pollution. However, fibers pollution is not limited to synthetics as all types of fibers are found in the
23 environment. According to the International Organization for Standardization (in ISO/TR 11827:2012
24 Textiles - Composition testing - Identification of fibers), fibers are classified into two main categories:
25 (i) man-made and (ii) natural fibers. Natural fibers are produced from crops or farming whereas man-
26 made fibers are manufactured from chemical manufacturing processes. Man-made fibers are divided
27 into artificial fibers, such as viscose (which come from cellulose, a natural polymer) and synthetic
28 fibers which mainly come from petroleum resources. Biobased synthetic fibers, which constitute less
29 than 1 % of the production rate (TextileExchange, 2018), will not be considered here.

30 From 1950 to 2015, ~600 Mt of polyester, polyamide, and acrylic fibers were dumped and
31 accumulated in the environment (Geyer et al., 2017). In 2017, the fiber production exceeded 100 Mt
32 for the first time and reached 105 Mt of which 68 % (71.5 Mt) was man-made *i.e.* artificial and
33 synthetic fibers. Polyester, polyamide, and acrylic fibers are the most produced synthetic fibers,
34 accounting for 62 % of the global fiber production (TextileExchange, 2018). Significant leaks to the
35 environment occur owing to wear and tear of textiles and synthetic products. Besides synthetic fibers,
36 artificial and natural fibers have been reported to significantly pollute the environment as microscopic
37 litter, particularly in biota matrices (Lusher et al., 2013; Remy et al., 2015; Rochman et al., 2015;
38 Zhao et al., 2016). Artificial and natural fibers can behave as pollutant vectors (Zhao et al., 2016) and
39 further research is needed to study their impact on the environment.

40 In microplastic studies, fibers < 5 mm are generally categorized as microfibers even though fibers of
41 this size limit is not always rigorously used (Arthur et al., 2009; Frias and Nash, 2019).

42 Quantitatively, fibers were reported as the major component of microplastics or plastic-suspected
43 particles (compared with various shapes such as fragments), and have been found in oceans (Law et
44 al., 2010), rivers (Rillig, 2012), fish stomachs (Collard et al., 2015), atmospheric outfall (Dris et al.,
45 2016), sediments (Ng and Obbard, 2006) and recently, in bottled water (Welle and Franz, 2018). The

46 ubiquity of microfibers may have negative effects on aquatic and terrestrial biota particularly, by
47 reducing the energy budgets available in food as well as exposing species to pathogens or
48 contaminants and oxidative stress (Foley et al., 2018; Song et al., 2019; Watts et al., 2015).

49 Fibers have been found in every compartment of urban water *i.e.*, drinking water (Mintenig et al.,
50 2019; Pivokonsky et al., 2018), wastewater treatment plants (Magnusson and Norén, 2014; Talvitie et
51 al., 2015), sewage sludge (Lv et al., 2019; Mahon et al., 2017), and stormwater (Dris et al., 2018;
52 Piñon-Colin and al., 2020). Boucher and Friot, 2017 estimated that 35 % of microplastics released
53 into oceans comes from the laundry of synthetic textiles. Several studies have attributed significant
54 fiber releases to washing (De Falco et al., 2019; Hernandez et al., 2017; Napper and Thompson,
55 2016). However, fiber pollution is not limited to only washing as apparel and furnishing textiles
56 contribute significantly to fiber pollution throughout their life (Henry et al., 2019). Owing to the
57 various environmental matrices (biota, water, sediments, etc.) fiber extraction and quantification in
58 the environment have proved to be scientific challenges. This variety of matrices include different
59 organic matter (OM) and mineral matter. Moreover, fiber quantification requires the removal of OM
60 and mineral matter without fiber degradation. Therefore, various protocols have been developed to
61 this end. Mineral matter is commonly removed by density separations whereas OM is commonly
62 removed by digestion protocols. Digestion protocols commonly used in various studies are tested on
63 different types of matrices and different polymers. In most cases, polymers in the form of fragments
64 are tested. In all studies that have tested digestion protocols for microplastic extraction, only a few
65 have considered fibers (Cai et al., 2019; Hurley et al., 2018; Piarulli et al., 2019; Thiele et al., 2019).
66 Moreover, the considered fibers are mostly synthetics, even though significant amounts of natural
67 fibers have been reported from environmental samples (Zhao et al., 2016). Several reagents have been
68 assessed, *i.e.* acids like HCl or HNO₃ (Avio et al., 2015; Catarino et al., 2017; Cole et al., 2014), bases
69 like NaOH or KOH (Dehaut et al., 2016; Karami et al., 2017; Mintenig et al., 2017; Piarulli et al.,
70 2019; Thiele et al., 2019), oxidizing agents such as H₂O₂ (Dris et al., 2018; Hurley et al., 2018;
71 Mintenig et al., 2014; Nuelle et al., 2014), enzymes (collagenase, proteinase, etc.) (Cole et al., 2015;
72 Courtene-Jones et al., 2017; Löder et al., 2017; Mintenig et al., 2017; Piarulli et al., 2019), a

73 combination of some reagents presented above (Cai et al., 2019; Collard et al., 2015), and more
74 recently, Fenton's reagent (Hurley et al., 2018; Tagg et al., 2017) which is produced from an
75 oxidation reaction catalyzed with Fe^{2+} ions commonly used in wastewater treatments (Kuo, 1992).

76 Acids seemed too aggressive for fragments (Avio et al., 2015), particularly for polyamide (PA),
77 polyethylene terephthalate (PET) and high-density polyethylene (HDPE) (Catarino et al., 2017).
78 Bases such as KOH seemed suitable (Dehaut et al., 2016; Karami et al., 2017) especially before 4 d at
79 room temperature (Piarulli et al., 2019). Damage was observed for polyester fibers exposed to 10 %
80 KOH after 4 d at room temperature (Piarulli et al., 2019). Impacts of 10 % KOH at 60 °C and 40 °C
81 after 48 h on fibers such as PET, polypropylene (PP), PA, acrylic, and rayon (viscose filaments) have
82 been recently assessed (Thiele et al., 2019). Rayon turned out to be dissolved at 60 °C but not at 40 °C
83 (Thiele et al., 2019). H_2O_2 is a common oxidizer used in digestion protocols but different microplastic
84 fragments turned out to be impacted such as PA 6.6, which is dissolved when exposed to H_2O_2 at
85 high temperatures (> 60 °C), PP, and polyethylene (PE) (Hurley et al., 2018; Nuelle et al., 2014;
86 Sujathan et al., 2017). Fenton's reagent has recently been proposed as a highly effective in digestion
87 protocols with no degradation reported on tested polymers (mostly fragments) (Hurley et al., 2018;
88 Tagg et al., 2017). Only PET fibers were tested. Enzymatic protocols have also been reported to be
89 highly effective with no damage to polyester and polypropylene fibers (Piarulli et al., 2019).
90 However, these protocols are generally expensive. Less expensive enzymatic digestion protocols exist
91 but are generally time consuming (at least 6 d) (Mintenig et al., 2017). A combination of NaClO and
92 HNO_3 has proved to be aggressive for polyvinyl chloride (Collard et al., 2015). A combination of
93 H_2O_2 and KOH has proved to have a strong impact on natural and semi-synthetic fibers (Cai et al.,
94 2019).

95 The impact of digestion protocols on synthetic fibers is not the only problem; blends of synthetic and
96 nonsynthetic fibers have been found in samples. Owing to the growing concerns about their adverse
97 effects on ecosystems, reliable and robust protocols that preserve the integrity of all kinds of fibers, or
98 at least, a knowledge of which protocol(s) may have an impact on the various fibers is needed.

99 Almost no data is available on mass changes, mechanical degradations, and/or microscopic
100 modifications of fibers for the various digestion protocols. To fill this data gap, five different
101 digestion protocols were tested on seven different industrial raw fibers *i.e.*, three synthetic fibers, one
102 artificial fiber, and three natural fibers. To fill the knowledge gap highlighted above, changes in mass,
103 diameter, mechanical properties, and chemical dissolution after digestion protocols were evaluated
104 using five performance parameters: (i.) mass, (ii.) morphology, (iii.) tenacity, (iv.) elongation at break
105 and (v.) infrared spectra.

106 For reliable results, we tested fibers with a similar diameter to fibers commonly found in samples
107 collected from the environment. Because OM can be particularly diverse and our study only focused
108 on the impacts of digestion protocols on fibers and did not consider the digestion efficiency of OM,
109 we selected protocols previously tested on organic matter.

110 Currently available data on the impact of digestion protocols on fibers in their original state is
111 inadequate. To avoid parasitic chemical reactions, the most crucial chemical parameters were
112 precisely measured and controlled (volume, fiber type, temperature, and the composition of the
113 solution). Our samples were free of OM. In this manner, potential influence of OM on reactions was
114 avoided. As such, we observed impacts on fibers from only digestion protocols.

115 Various databases are commonly referred to when predicting reactions between polymers and
116 solvents, such as the Hildebrandt or the Hansen solubility parameters (Wypych, 2016). However,
117 parameters such as temperature, concentration, and reaction time are important factors that could
118 affect those predictions and necessitate the need for imposing an experimental validation procedure.

119 2. Material and methods

120 2.1. Prevention of microplastic contamination

121 Contamination mitigation was ensured using the following precautions:

- 122 • All the solutions used were preliminarily filtered on GF/D Whatman filters (Sigma Aldrich,
123 2.7 μm).

- 124 • All the glass vessels and filters were heated at 500 °C for 2 h before use. Vessels were then
125 rinsed with filtered water and filtered 50 % ethanol (96 %, technical). Plastic materials were
126 avoided and only 100 % cotton laboratory coats were worn.
- 127 • Fibers were stored in glass beakers covered by aluminum foils. Moreover, beakers were all
128 covered by aluminum foils during experiments.

129 2.2. Tested protocols

130 To be fit for operation, digestion protocols must be (i) easy to apply (in only one step), (ii) fast (less
131 than 48 h), and (iii) inexpensive. For the latter two, enzymes were not considered. Acids were also
132 avoided because important degradations were observed after acidic digestions (Avio et al., 2015;
133 Catarino et al., 2017). Five protocols were selected:

- 134 • Protocol 1: 50 ml of 10 % KOH (v/w) for 24 h at 40 °C adapted from Karami et al., 2017;
- 135 • Protocol 2: 50 ml of 10 % KOH (v/w) for 24 h at 60 °C adapted from Dehaut et al., 2016;
- 136 • Protocol 3: 50 ml of 1:4 diluted NaClO (La Croix ®, 3.6 w% of active chloride) for 1 night
137 (15 h) at room temperature (~20 °C) adapted from Collard et al., 2015;
- 138 • Protocol 4: 50 ml of 30 % H₂O₂ (v/v) for 48 h at 40 °C adapted from Mintenig et al., 2014;
- 139 • Protocol 5: 50 ml of Fenton's reagent for 2 h, using 33.3 ml of 30 % H₂O₂ (v/v) with 16.7 ml
140 of an iron(II) sulfate heptahydrate catalyst solution (20 g of FeSO₄·7H₂O dissolved in 1 L of
141 distilled water) acidified with sulfuric acid (H₂SO₄, pH = 3) adapted from Hurley et al., 2018.

142 Only temperature differed for Protocols 1 and 2. Fibers and particularly synthetic fibers, are known to
143 be sensitive to heat (Wypych, 2016). The tentative glass transition temperatures (T_g) for PET and PA
144 6.6 are close to 60 °C (tentative glass transition temperature for PET: 60–85 °C and for PA 6.6: 56–
145 70 °C (Wypych, 2016)), which means high temperatures (> 60 °C) can impact their structure.
146 Moreover, Thiele et al., 2019 observed a total dissolution of viscose when exposed to 10 % KOH at
147 60 °C for 48 h. Other works found polymer degradations owing to high temperatures (>70 °C)
148 (Munno et al., 2017). For these reasons, the impact of temperature was investigated. For Protocol 3,
149 contrary to the original protocol from Collard et al., 2015, digestion was reduced to a one-step process

150 to test NaClO potential impacts on fibers. Reagent impacts on fiber integrity for a combination of
151 reagents is complex. Moreover, a slightly lower concentration was tested in this study to reduce the
152 potential impacts on fibers. In this paper, Protocols 1 to 5 are denoted as follows: KOH 40 °C, KOH
153 60 °C, NaClO, H₂O₂, and Fenton.

154 2.3. Tested fibers

155 We tested widely available commercial raw fibers used for textile manufacture with worldwide
156 circulation (TextileExchange, 2018): three synthetics (polyethylene terephthalate (PET), polyamide
157 6.6 (PA 6.6), and polyacrylonitrile (acrylic)), one vegetal artificial (viscose), two vegetal natural
158 (cotton and flax), and one animal natural (wool). We selected raw fibers in our tests for three main
159 reasons:

- 160 • Studies on mass variations require large amounts of fibers (at least 800 mg per sample).
161 However, collecting large amounts of environmental fibers would have been complicated
162 because the extraction of environmental fibers is time consuming. Practically, only a few mg
163 would have been extracted.
- 164 • Artificial weathering would have been appropriate but it raises two issues: (i) which method
165 should be considered as the most representative for environmental fibers analyses (UV
166 exposure, mechanical or biological degradation, hydrolysis or a combination of these
167 methods?); (ii) no current standards exist concerning acceptable thresholds for parameters
168 used during artificial weathering.
- 169 • Raw fibers are supposed to be more resistant than environmental fibers. Thus, if a digestion
170 protocol affects raw fibers, it need not be tested on environmental fibers.

171 For these reasons, we selected raw fibers as reference materials as they provided a basis for a better
172 assessment and better reproducibility. We acquired the raw fibers from GEMTEX (textile materials
173 engineering laboratory, Roubaix, France), in the form of filaments with an initial length of ~10 cm.
174 Those fibers correspond to commonly used materials before industrial spinning processes. We
175 characterized these fibers before and after subjecting them to digestion protocols. As the fibers are

176 commercial raw fibers, they include additives. We were not able to obtain specific information about
177 the additives from the supplier. Because fibers from environmental samples also include additives
178 (which are generally unknown) and as the final objective of the study is to obtain a method suitable
179 for environmental samples, it is appropriate to test this methodology on commercial raw fibers with
180 unknown additives and not on laboratory-prepared ones, to achieve a higher representativity.

181 2.4. Performance parameters and experimental design

182 Digestion protocols were carried out following the steps below: for a given digestion protocol, $200 \pm$
183 20 mg of each fiber (800 ± 20 mg for mass variation assessment, to ensure a higher representativity)
184 were cut using cleaned scissors (fiber length from 1 mm to 5 cm) and plunged into 50 ml of reagent
185 (KOH, H_2O_2 , NaClO, or Fenton's reagent) in a beaker using metallic clamps. 200 ml of reagent was
186 used for mass variation assessment as a higher fiber mass was used to test this parameter (except for
187 Fenton's reagent, for which 100 ml was used to avoid violent reaction). Scissors and clamps were
188 rinsed thoroughly between samples with filtered water followed by filtered 50 % ethanol (96 %,
189 technical) to avoid contamination. Reaction occurred in beakers and on a heating plate IKA® RT, 15-
190 15 position (when heating was needed) at the required temperature (temperature precision: ± 2 °C),
191 without stirring. Temperatures were regularly checked using a checktemp 1 HI 98509 Hanna
192 Instruments® precision thermometer. After the allotted time, the heating was stopped and the
193 solutions containing the fibers were filtered on GF/D Whatman filters (Sigma Aldrich, porosity:
194 $2.7 \mu\text{m}$ and $\text{Ø } 90$ mm). Filters that contained digested fibers were stored in glass Petri dishes, put in a
195 desiccator for 48 h, and then dried in an oven at 40 °C for 48 h. Finally, fibers were put in a controlled
196 atmosphere (20 °C, 65 % relative humidity) for at least 24 h. The parameters of the fibers before and
197 after digestion are presented in Results and discussion.

198 2.4.1. Mass variation

199 For mass variation, each digestion protocol was tested three times, *i.e.*, for each digestion protocol,
200 three different fiber batches of 800 mg of each fiber type underwent the same digestion protocol. The

201 fibers were weighed before being used in the digestion protocols. When dry, the fibers were weighed
202 using a Sartorius® CPA225D precision balance (± 0.01 mg).

203 2.4.2. Morphological aspects

204 The fibers were longitudinally and cross-sectionally observed using an optical microscope MOTIC
205 B1-223, at three magnifications (x10, x40, x60). For longitudinal observations, it was necessary to
206 isolate a few fibers and put them into two glass slides. After the longitudinal observations, a small
207 number of fibers were parallelized and cut using a microtome (Hills Inc.), for cross-sectional
208 observations. When damages were detected or suspected, fibers were pasted on an aluminum stub
209 with a double face adhesive then coated with a uniform platinum film by vacuum evaporation (Jeol
210 JFC-1100E) and observed using a Scanning Electron Microscope (SEM) (Jeol 6301F) fitted with an
211 X-ray Energy Dispersive Spectrometer (Silicon Drift X-Max 80 mm² detector and Aztec Advanced-
212 INCA350 analyzer, Oxford Instruments). To observe damages and characterize deposits on fibers,
213 secondary electron analysis and X-ray analysis were performed, respectively.

214 2.4.3. Mechanical properties

215 The tenacity and elongation of the fibers at break were assessed. Tenacity, as shown in Equation 1,
216 corresponds to the ratio between the maximum longitudinal strength that a fiber can endure, and its
217 linear density:

218 Equation 1. Definition of tenacity (cN/Tex)

$$219 \text{ Tenacity } \left(\frac{\text{cN}}{\text{Tex}} \right) = \frac{\text{Maximum tensile strength (cN)}}{\text{Linear density (Tex)}} \quad (1)$$

220 The maximum tensile strength of fibers was assessed following the NF EN ISO 5079 standard on a
221 tensile testing machine (Zwick (1456)); the cell force used was 10 N, with a preload of 0.2 N/m². All
222 the tests were carried out at standard atmosphere conditions (20 ± 2 °C; HR 65 ± 5 %). The lengths of
223 the samples were 20 mm and the deformation rate were 20 mm/min, with the preload.

224 Linear density also called fiber count usually expressed in Tex or dTex (10^{-7} kg. m⁻¹), is the ratio
225 between mass and length. Two different methods were used for linear density measurement: (i)
226 measurement of radius of the fibers and (ii) vibroscope measurements (only for synthetic fibers). The
227 first method is a direct measurement of fiber radius using a microscope. Linear density is shown in
228 Equation 2.

229 Equation 2. Linear density depending on fiber radius

$$230 \text{ Linear density} = 10^{-7} \rho \pi r^2 \quad (2)$$

231 with linear density in dTex; ρ = density in kg. m⁻³; and r = fiber radius in m

232 30 radius measurements were taken for each fiber (digested and nondigested) except for PET and
233 acrylic as they were too dark for direct observation of their fiber radius. To solve this problem, PET
234 and acrylic fibers were mixed with light-colored fibers (wool) and their radii compared. 10 radius
235 measurements were taken for the dark-colored fibers. The second method was only applied to
236 synthetic fibers (PET, PA 6.6, and acrylic). It required the use of a vibroscope (Lenzing instrument).
237 For this method, 10 measurements were taken.

238 Elongation at break is the ratio between the initial length and the maximum length before the rupture
239 of the fiber. Elongation at break and tenacity were measured at the same time using the tensile test
240 bench at the same conditions outlined above.

241 For synthetic fibers (PET, PA 6.6, and acrylic), at least 5 and up to 30 tensile tests were performed.
242 Owing to handling difficulties, elongation at break and tenacity measurements were adapted for
243 artificial and natural fibers (samples length was 10 mm) and up to six tensile tests were performed.

244 2.4.4. Infrared spectra

245 To study the spectral modifications of the different fibers after digestion, fibers were chemically
246 characterized using a Fourier-Transform Infrared (FTIR) spectroscope (Thermo Scientific® Nicolet
247 iN10 MX) in transmission mode. A few fibers were put on Whatman® anodisc inorganic filter

248 membrane (porosity: 0.2 μm , \O 25 mm) and analyzed using the same parameters for each fiber type.
249 The detector used was a Thermo Scientific® MCT/A Cooled 25 mm detector, (spectral range of 4000
250 to 1200 cm^{-1} to avoid interferences with the anodisc filter, detection time of 12 seconds (64 scans) in
251 absorbance mode). Spectroscope aperture used was 20 μm in width and 20 μm in height. For each
252 experiment, six infrared spectra on six different fibers were collected. To compare nondigested and
253 digested fibers, an auto-baseline correction was applied to all infrared spectra. Then, for a given fiber
254 type, an average of the six spectra was applied. Digested fibers spectra were compared to nondigested
255 ones using the average spectra and the correlation comparison software “Q-check” (Thermo
256 Scientific®), which gives a percentage of correlation between two spectra by comparing all the
257 different peaks of both infrared spectra.

258 2.5. Evaluation of digestion protocols impacts

259 To evaluate the impact of digestion protocols, impact indicators were defined for variations of
260 morphological aspects, mass, tenacity, elongation at break, and infrared spectra correlations. To
261 ensure a better comparison and to avoid statistical bias owing to extreme values, median values were
262 used instead of mean values. For a given parameter value, a score was given depending on the impact
263 indicators previously defined: 0 for “no data”, 1 for “not affected”, 2 for “slightly affected”, 3 for
264 “affected”, and 4 for “highly affected”. All impact indicators and scores for each parameter are
265 reported in Table 1. For example in Table 1, for mass variation, fibers were observed to be slightly
266 affected (score = 2) when mass variation ranged between 5-10 %. They were observed to be highly
267 affected (score = 4) when mass variation reached beyond 25 %. The same indicator values were used
268 for tenacity and elongation at break measurements. It is important to note that when fibers were too
269 brittle to be handled, the maximum score for tenacity and elongation at break was attributed. For
270 morphological impacts, different key indices were considered for structural modifications such as
271 radius reduction, fiber tear, modification of rugosity, flattening, and color variation.

Parameters	Score	Indicator
Mass variation	0	No data
	1	Ranges from 5 to -5 %
	2	Ranges from 10 to -10 %
	3	Ranges from 25 to -25 %
	4	> 25 or < -25 %
Morphological aspects	0	No data
	1	No visible modification
	2	Slight modifications are visible
	3	Degradations and/or structural changes are visible
	4	The fiber structure is highly degraded
Tenacity	0	No data
	1	10 % decrease
	2	20 % decrease
	3	50 % decrease
	4	> 50 % decrease
Elongation at break	0	No data
	1	10 % decrease
	2	20 % decrease
	3	50 % decrease
	4	> 50 % decrease
FTIR Spectral comparison	0	No data
	1	Correlation between 100 and 90 %
	2	Correlation between 90 and 80 %
	3	Correlation between 80 and 60 %
	4	Correlation below 60 %

273 Table 1. Impact indicators and scores for each parameter

274 3. Results and discussion

275 3.1. Mass variation

276 Median values for mass variations of all the fibers after the different digestion protocols are reported
277 in supplementary data (Table S5). Considering the balance precision (0.01 mg) and the initial fiber
278 mass (800 ± 20 mg), the significance of the results is confirmed when mass variations are higher than
279 0.5 %. However, after KOH 40 °C, KOH 60 °C, and Fenton, mass gains of 5–10 % are observed for
280 almost all the fibers. This is most likely attributed to potassium or iron deposits on fibers which were

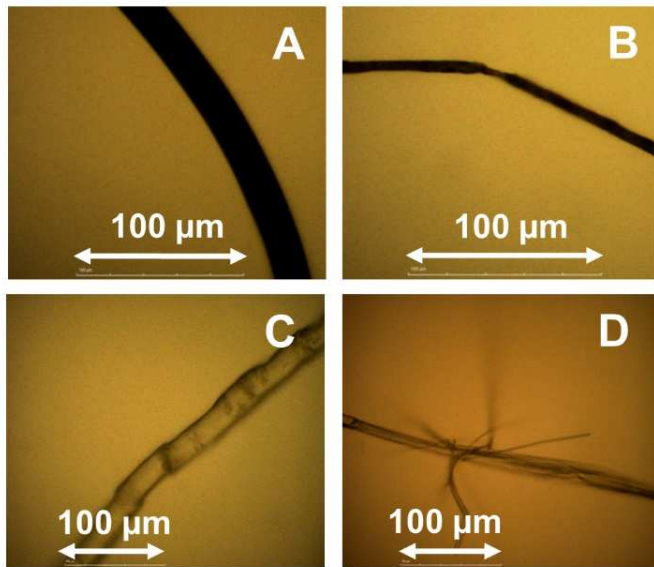
281 observed on fibers via scanning electron microscopy (see supplementary data, Figure S1). Owing to
282 the deposits observed, it is important to be vigilant on mass variations. For this reason, the
283 interpretation of results focused on important mass variations (> 20 %, in absolute value).

284 Wool is dissolved after KOH 40 °C, KOH 60 °C, and strongly affected after NaClO. As such it was
285 not considered in the other tests except in H₂O₂ and Fenton's reagent). Wool is composed of proteins
286 (mostly keratin) known to be easily dissolved by various solvents (Lewin, 2006).

287 PET is strongly affected by KOH 60 °C, 65.6 % of mass loss (median value) is observed for PET
288 fibers, owing to fiber degradation. PET is known to have poor resistance to alkalis (Wypych, 2016).
289 Nevertheless, this observation shows the importance of temperature as KOH 40 °C does not affect
290 PET mass. For PET, temperatures close to T_g facilitate solvent migration in amorphous zones, which
291 eventually provokes fiber dissolution. Viscose mass decreases after H₂O₂ (~20 % mass loss).

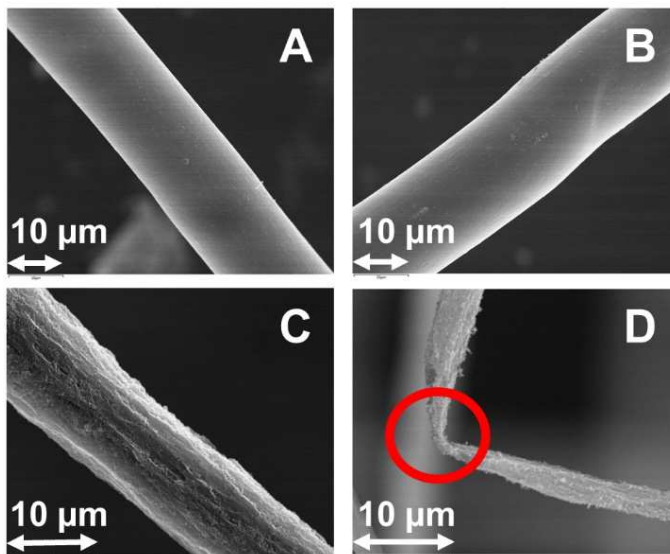
292 3.2. Morphological aspects

293 Except for PET and flax after specific digestion protocols, no other morphological alterations are
294 revealed by the optical microscope. PET is highly altered after KOH 60 °C (see Figure 1) whereas no
295 degradation is observed for KOH 40 °C. After KOH 60 °C PET diameter decreases from 20 to
296 approximately 12 μm, but not consistently. Moreover, the shape of the fiber changes, from smooth to
297 coarse (Figure 1). From SEM images, Figure 2 confirms that PET is highly degraded after KOH 60
298 °C. The fibers are observed to reduce in radius from 20 μm before KOH 60 °C to less than 12 μm
299 after KOH 60 °C. Buckling zones are observed (see the red circle in Figure 2D). Buckling zones are
300 attributed to a decrease in the global mechanical properties of the fibers from frequent observations.
301 This hypothesis is confirmed by tenacity and elongation at break variations (see “mechanical
302 properties”). SEM images also confirm an increase of the surface roughness for the digested fibers.
303 KOH 60 °C on PET was repeated and another SEM analysis was performed on those fibers. We
304 observed similar degradation. This observation confirms our first hypothesis that PET could be
305 degraded with temperatures close to or above 60 °C.



306

307 Figure 1. Optical microscope images (x40); A: PET before digestion; B: PET after KOH 60
 308 °C; C: Flax hull before digestion; D: Flax hull after NaClO.



309

310 Figure 2. SEM images obtained by secondary electron analysis of PET fibers before (A and
 311 B) and after (C and D) KOH 60 °C. The red circle shows a buckling zone.

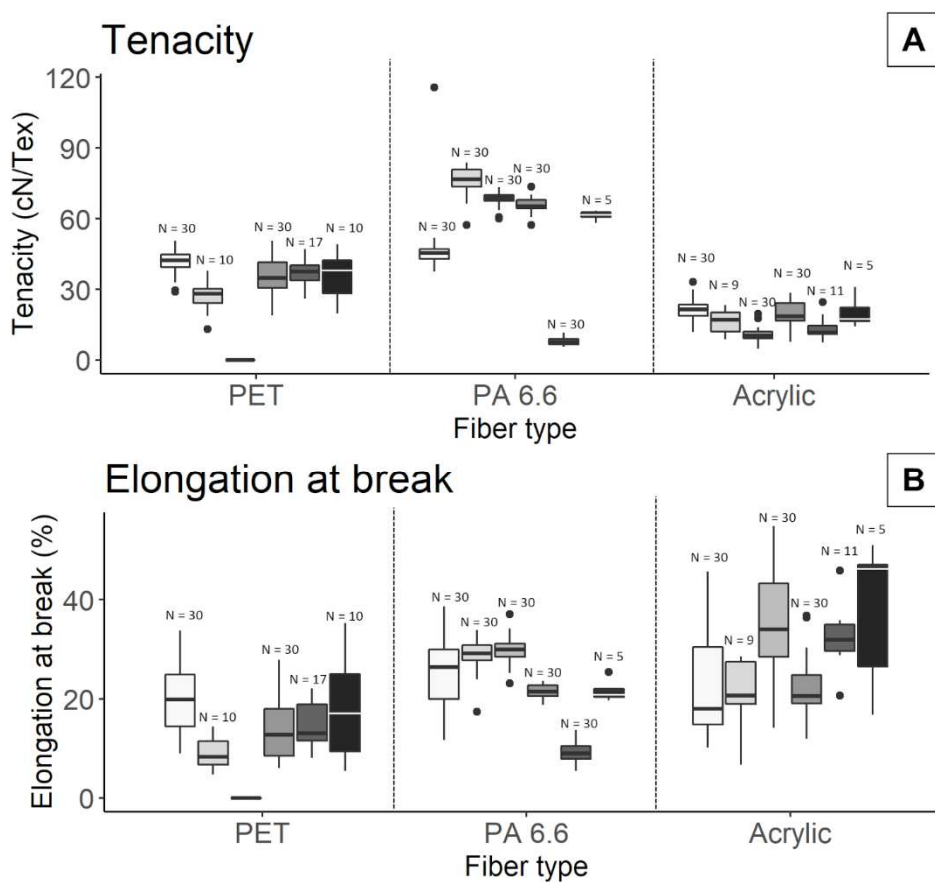
312 The flax cell wall is shattered by NaClO as shown in Figure 1D. The NaClO probably dissolved a part
 313 of this cell wall during the digestion. This observation is confirmed by SEM (see supplementary data
 314 Figure S2).

315 Finally, iron and potassium depositions are observed and confirmed after Fenton, KOH 40 °C, and
 316 KOH 60 °C respectively, using X-ray analysis (Figure S1).

317 3.3. Mechanical properties

318 3.3.1. Synthetic fibers

319 Boxplots of tenacity and elongation at break for synthetic fibers before and after the different
 320 digestion protocols are presented in Figure 3.



321 Before dig. KOH 40°C KOH 60°C NaClO H₂O₂ Fenton

322 Figure 3. Boxplots of tenacity (A) and elongation at break (B) for synthetic fibers before
 323 digestion (noted “Before dig.”) and after the different digestion protocols. Black dots
 324 correspond to extreme values.

325 Statistical significance between the results before and after each digestion was tested using a Mann-
 326 Whitney-Wilcoxon test. P-values for tenacity and elongation at break are presented in Table 2.
 327 Significance is not confirmed for grayed-out values.

		PET	PA 6.6	Acrylic
KOH 40 °C	Tenacity	3.10E-05	5.60E-10	1.70E-02
	Elongation	6.80E-05	2.00E-02	9.60E-01
KOH 60 °C	Tenacity	-	5.60E-10	7.40E-10
	Elongation	-	3.70E-03	3.00E-04
NaClO	Tenacity	8.10E-04	5.60E-10	1.70E-01
	Elongation	1.50E-03	5.70E-02	5.20E-01
H₂O₂	Tenacity	5.50E-03	3.00E-11	3.90E-04
	Elongation	1.40E-02	4.10E-11	1.10E-02
Fenton	Tenacity	6.70E-02	1.00E-03	5.60E-01
	Elongation	4.60E-01	4.40E-04	3.20E-02

328 Table 2. P-values for tenacity and elongation at break values after Mann-Whitney-Wilcoxon
 329 test for each fiber and protocol (significance is not confirmed for grayed-out values)

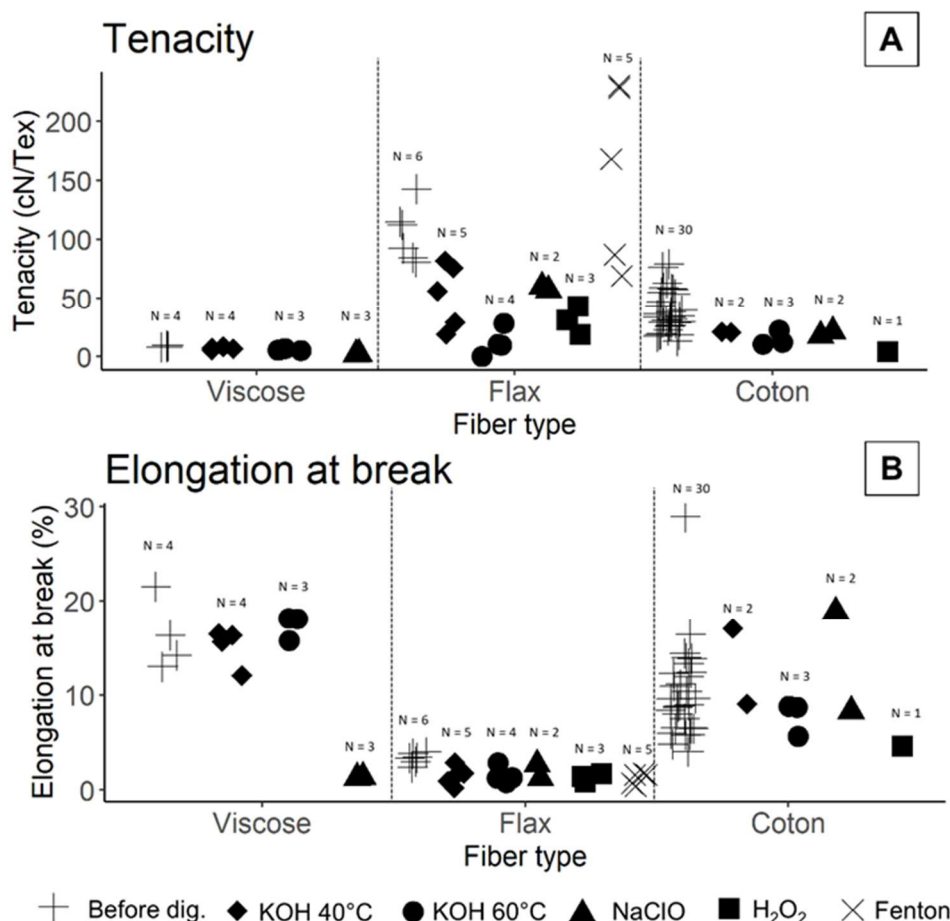
330 For PET, tenacity, and elongation at break median values decrease after each digestion protocol. This
 331 trend is more pronounced for PET which underwent KOH 40 °C. As for tenacity, PET after KOH 60
 332 °C was too brittle to be tested.

333 PA 6.6 presents unexpected behavior. For this fiber, increases of tenacity (which are significant) are
 334 observed for all protocols, to the exception of H₂O₂. Those increases are difficult to interpret. PA 6.6
 335 after H₂O₂ presents a significant decrease for both tenacity and elongation at break, showing a
 336 mechanical degradation.

337 For acrylic, tenacity slightly decreases after KOH 60 °C and H₂O₂. However, elongation at break is
 338 not affected the same way. For this parameter, values are globally stable or slightly increase.

340 3.3.2. Artificial and natural fibers

341 Tenacity and elongation at break for artificial and natural fibers before and after the different
 342 digestion protocols are presented in Figure 4.



343

344 Figure 4. Tenacity (A) and elongation at break (B) for natural and artificial fibers before
 345 digestion (noted “Before dig.”) and after the different digestion protocols

346 Owing to the number of tests (generally below 5 tests), statistical significance cannot be confirmed for
 347 artificial and natural fibers. However, different trends can be observed.

348 Viscose tenacity before digestion is particularly low (median value = 8.46 cN/Tex) compared to other
 349 fibers. Its tenacity decreases after KOH 40 °C (6.96 cN/Tex) and KOH 60 °C (5.42 cN/Tex). Even
 350 though this decrease might not be significant, it is more marked for NaClO (2.00 cN/Tex, a decrease
 351 of 76.3 %). For this fiber, elongation at break is stable after KOH 40 °C and KOH 60 °C. Elongation

352 at break seems however affected after NaClO, for which an important decrease is observed after these
353 tests (median value = 1.35 cN/Tex, a decrease of 91.2 %). After H₂O₂ and Fenton, viscose was too
354 brittle to be tested and broke at each manipulation with metallic clamps (even though, no degradation
355 is visible neither by optical microscope nor SEM).

356 For flax, KOH 40 °C, KOH 60 °C, NaClO, and H₂O₂ have an impact on tenacity. Elongation at break
357 generally decreases (~50 % decrease for median values of all digestions).

358 For cotton, 30 tests were performed before digestion. It was however not possible to reproduce as
359 many tests after digestions. For tenacity, values after digestions generally correspond to the lowest
360 values found before digestion, which could indicate a global decrease for all digestions. For
361 elongation at break, no trend can be observed. Only one test was performed after H₂O₂, owing to the
362 brittleness of cotton after this digestion.

363 3.3.3. Discussion regarding the changes in tenacity and elongation at break

364 Changes in tenacity and elongation at break after digestion protocols are attributed to chemical
365 resistance. According to Wypych (2016), PET has a poor resistance to alkalis which explains why its
366 tenacity and elongation at break decreased after KOH 40 °C and KOH 60 °C. A slight PET
367 dissolution may start at 40 °C, causing slight mechanical degradations. This dissolution is much
368 greater for KOH at 60 °C. Other digestion protocols have a lower impact.

369 PA 6.6 is known for its mechanical strength and its good chemical resistance to most common
370 solvents (Wypych, 2016). Increases in tenacity would imply a higher mechanical resistance to
371 traction. Because elongation at break is globally stable for nearly all protocols, the elasticity of PA 6.6
372 did not change. Even though results from PA 6.6 tests were unclear, there could be sorption
373 mechanisms between ions (K⁺, Na⁺, Cl⁻) and the amorphous zone of PA 6.6 as observed between
374 water molecules and polyamide fibers (Lewin, 2006; Puffr and Šebenda, 1967). These interactions
375 may have changed the mechanical properties of PA 6.6. For Fenton, more tests should be performed
376 to confirm these trends. On the contrary, mechanical degradation was observed after the H₂O₂. 30 %
377 H₂O₂ oxidized PA 6.6, this concentration is too high to maintain PA 6.6 integrity.

378 For acrylic, its tenacity and elongation at break are globally stable. However, its tenacity slightly
379 decreases after KOH and H₂O₂ resulting in a small impact. Its elongation at break varies within the
380 same range of values before and after all digestions. Acrylic is known to be resistant to many solvents,
381 which was confirmed by our test results (Wypych, 2016).

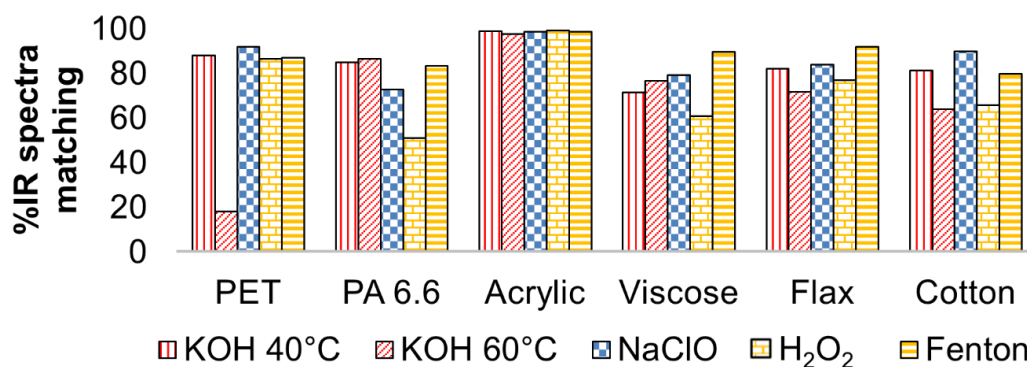
382 For viscose, its tenacity and elongation at break were impacted by NaClO. Moreover, H₂O₂ and
383 Fenton were too aggressive for this fiber. Viscose is known as a more brittle fiber owing to its
384 structure and manufacturing process (regenerated cellulose) (Wypych, 2016).

385 As opposed to cotton and viscose, flax is composed of hemicellulose and lignin in addition to
386 cellulose which could explain the observed decreases following different protocols. Lignin dissolution
387 may explain the degradations (confirmed on SEM for flax exposed to NaClO, see supplementary data
388 Figure S2).

389 Cotton has chemical resistance to many solvents which could explain why no particular impacts were
390 observed after digestion protocols (Lewin, 2006; Wypych, 2016).

391 3.4. Infrared spectra

392 Using Q-check software (see Material and methods), the correlation of infrared spectra of digested
393 and nondigested fibers were compared (Figure 5).



394
395 Figure 5. Matching percentages between nondigested and digested fibers infrared signals
396 for each fiber type and each digestion protocol. The comparison was performed with Q-
397 check from Thermo Scientific® analysis software.

398 PET after KOH 60 °C and PA 6.6 after H₂O₂ show the lowest correlation values of all studied fibers
399 (17.8 % and 50.7 % respectively). The low value of PET after KOH 60 °C is most likely attributable
400 to the reduction in diameter (from 20 μm to ~12 μm). Additionally, 10 μm generally corresponds to
401 the smallest sample size that can be analyzed by FTIR spectroscopy.

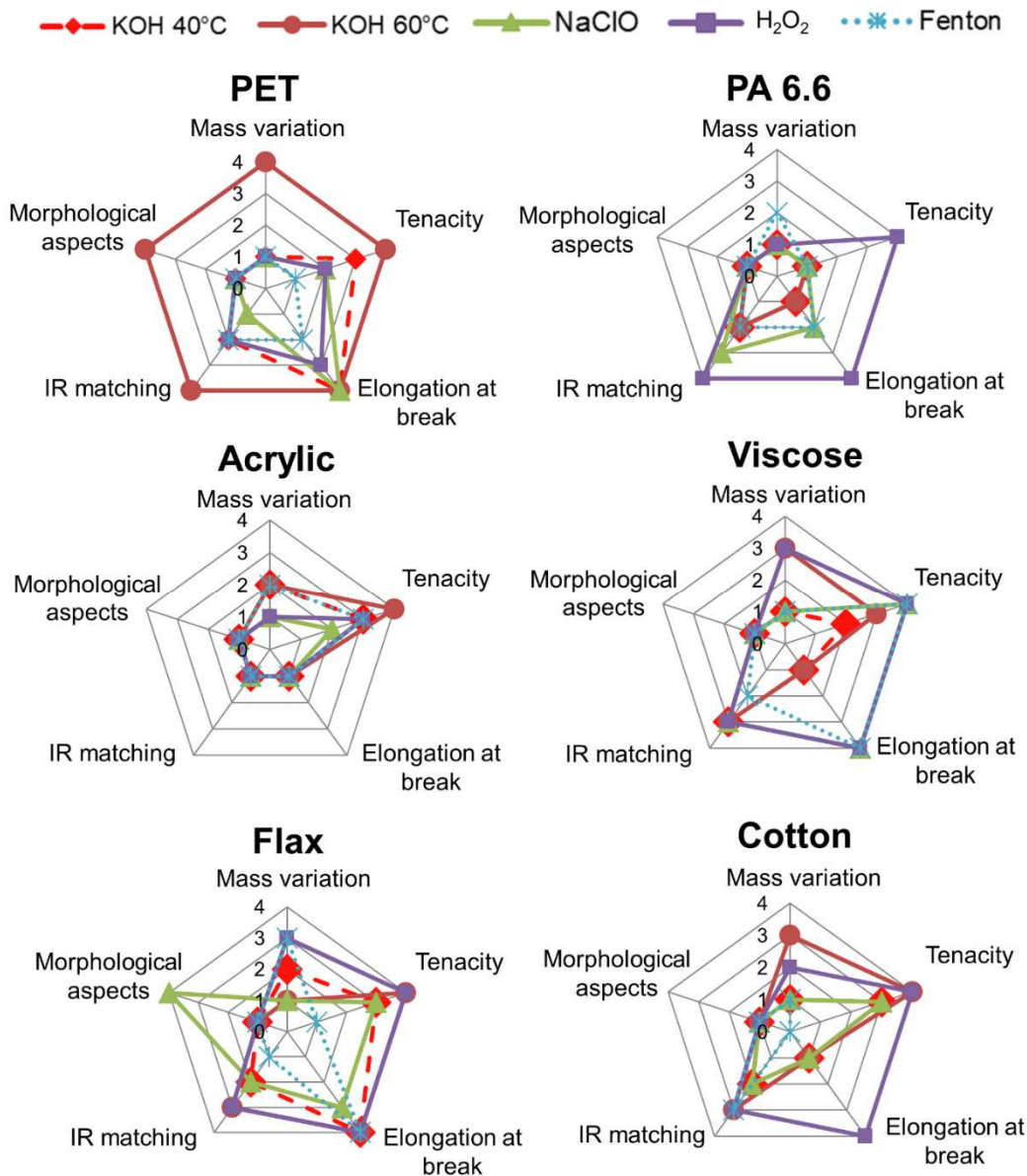
402 For these fibers, infrared spectra are available in supplementary data (Figure S3 and Figure S4). Most
403 of the digestions have an impact on the infrared signals of viscose, flax, and cotton, with most of the
404 correlation percentages lying between 60 and 80 %. Acrylic has almost no signal modifications for
405 any digestion protocol (all values were higher than 90 %). In terms of signal modification,
406 KOH 40 °C, NaClO, and Fenton are the most suitable digestion protocols for reducing the impacts on
407 infrared spectra.

408 3.5. Evaluation of digestion protocols impacts

409 By applying the different impact indicators previously defined, a score for each parameter value for
410 each tested fiber was obtained. Radar charts in Figure 6 present an overview of all the impacts
411 observed. Detailed variations of all parameters of each fiber after each digestion are reported in
412 supplementary data (Table S5).

413 According to Figure 6, acrylic is the most resistant fiber; its performance parameters are not
414 significantly impacted. Figure 6 shows that digestion impacts depend on fiber nature.

415 KOH 60 °C and H₂O₂ have the strongest impacts which, however, differ significantly. KOH 60 °C has
416 a targeted impact on PET. Additionally, all performance parameters highly impacted by KOH 60 °C
417 (see Figure 6). Mass variation in PET owing to degradation after KOH 60 °C (65.6 % of mass loss)
418 could lead to underestimations of weight if KOH 60 °C, for example, is followed by Pyr-GC-MS. To
419 a lesser extent, KOH 60 °C also impacts the mechanical properties of flax and cotton as well as
420 viscose mass. This is attributable to temperature as KOH 40 °C reduced those impacts, even though
421 tenacity and elongation at break are still affected (Figure 6). Surprisingly, viscose was not dissolved,
422 contrary to what Thiele et al., 2019 observed after KOH 60 °C.



423

424 Figure 6. Radar diagrams of the impacts of digestion protocols for each fiber type

425 H₂O₂ affects the mechanical properties (tenacity and elongation at break) and IR spectra of PA 6.6

426 and potentially viscose, flax, and cotton. Brittleness of these fibers after H₂O₂ has been observed

427 during handling. This brittleness could potentially lead to fiber fragmentation which could result in

428 counting errors and false estimations. H₂O₂ impacts on PA 6.6 support observations made by previous

429 works (Hurley et al., 2018; Nuelle et al., 2014; Sujathan et al., 2017) even though we did not observe

430 dissolution of PA 6.6. This could be attributed to the length of the used fibers (>1 mm and up to 5

431 cm). The observed impacts of this digestion could mainly be attributed to two parameters: (i)

432 concentration, (ii) the reaction time (48 h), or probably a combination of both. Previous works used
433 more diluted H₂O₂ solutions (Sujathan et al., 2017).

434 It is worth noting that our results do not prove fibers fragmentation during protocols. Rather, they
435 only compare the impact of digestion protocols on different fiber parameters. Our results form a basis
436 for developing a more suitable digestion protocol for fiber extraction.

437 KOH 40 °C, NaClO, and Fenton have the smallest impacts on fibers. Karami et al., 2017 showed an
438 increase in the recovery rate of microplastics and digestion efficiency when KOH 40 °C was used
439 instead of KOH 60 °C. Piarulli et al., 2019 showed PES fibers degraded after 4 d of exposure in KOH
440 1M at room temperature. More tests are needed to find out the optimum time and temperature for
441 KOH digestion, but 10 % KOH at 40 °C for 24 h is promising to be effective in maintaining fiber
442 integrity.

443 Apart from flax and viscose, NaClO does not impact most of the parameters of the fibers. However,
444 the efficiency of this protocol on OM should be assessed as it is commonly combined with HNO₃
445 (Collard et al., 2015).

446 Finally , Fenton shows high efficiency for OM removal (Hurley et al., 2018; Tagg et al., 2017) with
447 small impacts on all tested fibers to the exception of viscose mechanical properties. This protocol
448 tends to be a suitable digestion protocol for fragments and fibers analysis. This could be explained by
449 the short reaction time (reaction ended in 15 minutes, although we let the reaction occur for 2 h)
450 without additional heating. However, an iron deposition was observed on GF/D filters, which may
451 complicate the analysis of microplastics, particularly counting. Iron concentration seems too high and
452 could be reconsidered to avoid those deposits. However, iron deposits have no influence on infrared
453 spectra (Figure 5).

454 To the exception of wool, results showed the relatively high resistance of natural fibers. This
455 observation supports the need of fiber characterization after digestion protocols. More techniques
456 should be developed to distinguish synthetic, semi synthetic and natural fibers.

457 Distinction between man-made cellulosic (e.g. viscose) and natural cellulosic fibers (e. g. cotton, flax)
458 in environmental samples is still a scientific challenge since degraded cellulosic fibers are generally
459 difficult to differentiate (Cai et al., 2019; Remy et al., 2015; Zhu et al., 2019). Thus, fiber
460 classification may be reconsidered for environmental fibers by distinguishing: (i) synthetic fibers, (ii)
461 cellulosic fibers and (iii) proteinaceous fibers which mainly come from animals. This new
462 classification could help for a better comparison between samples.

463 4. Conclusion

464 10 % KOH 60 °C for 24 h and 30 % H₂O₂ 40 °C for 48 h have the strongest impacts on raw fibers
465 particularly synthetics and should be avoided for microfibers analysis. 10 % KOH 40 °C for 24 h, 1:4
466 diluted NaClO for one night (15 h) at room temperature (~ 20 °C) and Fenton's reagent are more
467 appropriate to maintain fibers integrity.

468 The tests within this study are performed on industrial raw fibers with no weathering. More tests
469 should be applied on weathered or artificially weathered fibers to assess digestion impacts on fibers.

470 Moreover, parameters could probably modify fiber stability towards digestion protocols, such as: (i)
471 formulation parameters (molar mass, additives...) and (ii) proceeding parameters (crystallinity,
472 specific surface area...). In the future, more data should be collected on the impacts of those
473 parameters.

474 5. Acknowledgment

475 This work was supported by the French ministry for the ecological and inclusive transition; the OPUR
476 project; the PIREN Seine project and Ecole des Ponts Paritech.

- 478 Arthur, C., Baker, J., Bamford, H., 2009. Proceedings of the International Research Workshop on the
479 Occurrence, Effects and Fate of Microplastic Marine Debris. Presented at the National
480 Oceanic and Atmospheric Administration Technical Memorandum NOS-OR&R-30.
- 481 Avio, C.G., Gorbi, S., Regoli, F., 2015. Experimental development of a new protocol for extraction
482 and characterization of microplastics in fish tissues: First observations in commercial species
483 from Adriatic Sea. *Mar. Environ. Res., Particles in the Oceans: Implication for a safe marine*
484 *environment* 111, 18–26. <https://doi.org/10.1016/j.marenvres.2015.06.014>
- 485 Boucher, J., Friot, D., 2017. Primary microplastics in the oceans. IUCN.
486 <https://doi.org/10.2305/IUCN.CH.2017.01.en>
- 487 Cai, H., Du, F., Li, L., Li, B., Li, J., Shi, H., 2019. A practical approach based on FT-IR spectroscopy
488 for identification of semi-synthetic and natural celluloses in microplastic investigation. *Sci.*
489 *Total Environ.* 669, 692–701. <https://doi.org/10.1016/j.scitotenv.2019.03.124>
- 490 Catarino, A.I., Thompson, R., Sanderson, W., Henry, T.B., 2017. Development and optimization of a
491 standard method for extraction of microplastics in mussels by enzyme digestion of soft
492 tissues. *Environ. Toxicol. Chem.* 36, 947–951. <https://doi.org/10.1002/etc.3608>
- 493 Cole, M., Webb, H., Lindeque, P.K., Fileman, E.S., Halsband, C., Galloway, T.S., 2015. Isolation of
494 microplastics in biota-rich seawater samples and marine organisms. *Sci. Rep.* 4.
495 <https://doi.org/10.1038/srep04528>
- 496 Cole, M., Webb, H., Lindeque, P.K., Fileman, E.S., Halsband, C., Galloway, T.S., 2014. Isolation of
497 microplastics in biota-rich seawater samples and marine organisms. *Sci. Rep.* 4.
498 <https://doi.org/10.1038/srep04528>
- 499 Collard, F., Gilbert, B., Eppe, G., Parmentier, E., Das, K., 2015. Detection of Anthropogenic Particles
500 in Fish Stomachs: An Isolation Method Adapted to Identification by Raman Spectroscopy.
501 *Arch. Environ. Contam. Toxicol.* 69, 331–339. <https://doi.org/10.1007/s00244-015-0221-0>
- 502 Courtene-Jones, W., Quinn, B., Murphy, F., Gary, S.F., Narayanaswamy, B.E., 2017. Optimisation of
503 enzymatic digestion and validation of specimen preservation methods for the analysis of
504 ingested microplastics. *Anal Methods* 9, 1437–1445. <https://doi.org/10.1039/C6AY02343F>
- 505 De Falco, F.D., Pace, E.D., Cocca, M., Avella, M., 2019. The contribution of washing processes of
506 synthetic clothes to microplastic pollution. *Sci. Rep.* 9, 6633. <https://doi.org/10.1038/s41598-019-43023-x>
- 508 Dehaut, A., Cassone, A.-L., Frère, L., Hermabessiere, L., Himber, C., Rinnert, E., Rivière, G.,
509 Lambert, C., Soudant, P., Huvet, A., Duflos, G., Paul-Pont, I., 2016. Microplastics in seafood:
510 Benchmark protocol for their extraction and characterization. *Environ. Pollut.* 215, 223–233.
511 <https://doi.org/10.1016/j.envpol.2016.05.018>
- 512 Dris, R., Gasperi, J., Saad, M., Mirande, C., Tassin, B., 2016. Synthetic fibers in atmospheric fallout:
513 A source of microplastics in the environment? *Mar. Pollut. Bull.* 104, 290–293.
514 <https://doi.org/10.1016/j.marpolbul.2016.01.006>
- 515 Dris, R., Gasperi, J., Tassin, B., 2018. Sources and Fate of Microplastics in Urban Areas: A Focus on
516 Paris Megacity. *Freshw. Microplastics* 69–83. https://doi.org/10.1007/978-3-319-61615-5_4
- 517 Foley, C.J., Feiner, Z.S., Malinich, T.D., Höök, T.O., 2018. A meta-analysis of the effects of exposure
518 to microplastics on fish and aquatic invertebrates. *Sci. Total Environ.* 631–632, 550–559.
519 <https://doi.org/10.1016/j.scitotenv.2018.03.046>
- 520 Frias, J.P.G.L., Nash, R., 2019. Microplastics: Finding a consensus on the definition. *Mar. Pollut.*
521 *Bull.* 138, 145–147. <https://doi.org/10.1016/j.marpolbul.2018.11.022>
- 522 Geyer, R., Jambeck, J.R., Law, K.L., 2017. Production, use, and fate of all plastics ever made. *Sci.*
523 *Adv.* 3. <https://doi.org/10.1126/sciadv.1700782>
- 524 Henry, B., Laitala, K., Klepp, I.G., 2019. Microfibres from apparel and home textiles: Prospects for
525 including microplastics in environmental sustainability assessment. *Sci. Total Environ.* 652,
526 483–494. <https://doi.org/10.1016/j.scitotenv.2018.10.166>
- 527 Hernandez, E., Nowack, B., Mitrano, D.M., 2017. Polyester Textiles as a Source of Microplastics
528 from Households: A Mechanistic Study to Understand Microfiber Release During Washing.
529 *Environ. Sci. Technol.* 51, 7036–7046. <https://doi.org/10.1021/acs.est.7b01750>

530 Hurley, R.R., Lusher, A.L., Olsen, M., Nizzetto, L., 2018. Validation of a Method for Extracting
531 Microplastics from Complex, Organic-Rich, Environmental Matrices. *Environ. Sci. Technol.*
532 52, 7409–7417. <https://doi.org/10.1021/acs.est.8b01517>

533 Karami, A., Golieskardi, A., Choo, C.K., Romano, N., Ho, Y.B., Salamatinia, B., 2017. A high-
534 performance protocol for extraction of microplastics in fish. *Sci. Total Environ.* 578, 485–
535 494. <https://doi.org/10.1016/j.scitotenv.2016.10.213>

536 Kuo, W.G., 1992. Decolorizing dye wastewater with Fenton’s reagent. *Water Res.* 26, 881–886.
537 [https://doi.org/10.1016/0043-1354\(92\)90192-7](https://doi.org/10.1016/0043-1354(92)90192-7)

538 Larkin, P., 2011. *Infrared and Raman Spectroscopy: Principles and Spectral Interpretation*. Elsevier
539 Science.

540 Law, K.L., Morét-Ferguson, S., Maximenko, N.A., Proskurowski, G., Peacock, E.E., Hafner, J.,
541 Reddy, C.M., 2010. Plastic accumulation in the North Atlantic subtropical gyre. *Science* 329,
542 1185–1188. <https://doi.org/10.1126/science.1192321>

543 Lewin, M., 2006. *Handbook of Fiber Chemistry*. CRC Press.

544 Löder, M.G.J., Imhof, H.K., Ladehoff, M., Löschel, L.A., Lorenz, C., Mintenig, S., Piehl, S.,
545 Primpke, S., Schrank, I., Laforsch, C., Gerdt, G., 2017. Enzymatic Purification of
546 Microplastics in Environmental Samples. *Environ. Sci. Technol.* 51, 14283–14292.
547 <https://doi.org/10.1021/acs.est.7b03055>

548 Lusher, A.L., McHugh, M., Thompson, R.C., 2013. Occurrence of microplastics in the
549 gastrointestinal tract of pelagic and demersal fish from the English Channel. *Mar. Pollut. Bull.*
550 67, 94–99. <https://doi.org/10.1016/j.marpolbul.2012.11.028>

551 Lv, X., Dong, Q., Zuo, Z., Liu, Y., Huang, X., Wu, W.-M., 2019. Microplastics in a municipal
552 wastewater treatment plant: Fate, dynamic distribution, removal efficiencies, and control
553 strategies. *J. Clean. Prod.* 225, 579–586. <https://doi.org/10.1016/j.jclepro.2019.03.321>

554 Magnusson, K., Norén, F., 2014. Screening of microplastic particles in and down-stream a wastewater
555 treatment plant.

556 Mahon, A.M., O’Connell, B., Healy, M.G., O’Connor, I., Officer, R., Nash, R., Morrison, L., 2017.
557 Microplastics in Sewage Sludge: Effects of Treatment. *Environ. Sci. Technol.* 51, 810–818.
558 <https://doi.org/10.1021/acs.est.6b04048>

559 Mintenig, S., Int-Veen, I., Löder, M., Gerdt, G., 2014. Mikroplastik in ausgewählten Kläranlagen des
560 Oldenburgisch - Ostfriesischen Wasserverbandes (OOWV) in Niedersachsen. Alfred-
561 Wegener-Inst. Helmholtz-Zent. Für Polar- Meeresforsch.

562 Mintenig, S.M., Int-Veen, I., Löder, M.G.J., Primpke, S., Gerdt, G., 2017. Identification of
563 microplastic in effluents of waste water treatment plants using focal plane array-based micro-
564 Fourier-transform infrared imaging. *Water Res.* 108, 365–372.
565 <https://doi.org/10.1016/j.watres.2016.11.015>

566 Mintenig, S.M., Löder, M.G.J., Primpke, S., Gerdt, G., 2019. Low numbers of microplastics detected
567 in drinking water from ground water sources. *Sci. Total Environ.* 648, 631–635.
568 <https://doi.org/10.1016/j.scitotenv.2018.08.178>

569 Munno, Helm Paul A., Jackson Donald A., Rochman Chelsea, Sims Alina, 2017. Impacts of
570 temperature and selected chemical digestion methods on microplastic particles. *Environ.*
571 *Toxicol. Chem.* 37, 91–98. <https://doi.org/10.1002/etc.3935>

572 Napper, I.E., Thompson, R.C., 2016. Release of synthetic microplastic plastic fibres from domestic
573 washing machines: Effects of fabric type and washing conditions. *Mar. Pollut. Bull.* 112, 39–
574 45. <https://doi.org/10.1016/j.marpolbul.2016.09.025>

575 Ng, K.L., Obbard, J.P., 2006. Prevalence of microplastics in Singapore’s coastal marine environment.
576 *Mar. Pollut. Bull.* 52, 761–767. <https://doi.org/10.1016/j.marpolbul.2005.11.017>

577 Nuelle, M.-T., Dekiff, J.H., Remy, D., Fries, E., 2014. A new analytical approach for monitoring
578 microplastics in marine sediments. *Environ. Pollut.* 184, 161–169.
579 <https://doi.org/10.1016/j.envpol.2013.07.027>

580 Piarulli, S., Scapinello, S., Comandini, P., Magnusson, K., Granberg, M., Wong, J.X.W., Sciutto, G.,
581 Prati, S., Mazzeo, R., Booth, A.M., Airolti, L., 2019. Microplastic in wild populations of the
582 omnivorous crab *Carcinus aestuarii*: A review and a regional-scale test of extraction methods,
583 including microfibrils. *Environ. Pollut.* 251, 117–127.
584 <https://doi.org/10.1016/j.envpol.2019.04.092>

585 Piñon-Colin, T. de J., al., 2020. Microplastics in stormwater runoff in a semiarid region, Tijuana,
586 Mexico. *Sci. Total Environ.* 704, 135411. <https://doi.org/10.1016/j.scitotenv.2019.135411>

587 Pivokonsky, M., Cermakova, L., Novotna, K., Peer, P., Cajthaml, T., Janda, V., 2018. Occurrence of
588 microplastics in raw and treated drinking water. *Sci. Total Environ.* 643, 1644–1651.
589 <https://doi.org/10.1016/j.scitotenv.2018.08.102>

590 Puffr, R., Šebenda, J., 1967. On the Structure and Properties of Polyamides. XXVII.† The Mechanism
591 of Water Sorption in Polyamides. *J. Polym. Sci. Part C Polym. Symp.* 16.
592 <https://doi.org/10.1002/polc.5070160109>

593 Remy, F., Collard, F., Gilbert, B., Compère, P., Eppe, G., Lepoint, G., 2015. When Microplastic Is
594 Not Plastic: The Ingestion of Artificial Cellulose Fibers by Macrofauna Living in Seagrass
595 Macrophytodetritus. *Environ. Sci. Technol.* 49, 11158–11166.
596 <https://doi.org/10.1021/acs.est.5b02005>

597 Rillig, M.C., 2012. Microplastic in Terrestrial Ecosystems and the Soil? *Environ. Sci. Technol.* 46,
598 6453–6454. <https://doi.org/10.1021/es302011r>

599 Rochman, C.M., Tahir, A., Williams, S.L., Baxa, D.V., Lam, R., Miller, J.T., Teh, F.-C., Werorilangi,
600 S., Teh, S.J., 2015. Anthropogenic debris in seafood: Plastic debris and fibers from textiles in
601 fish and bivalves sold for human consumption. *Sci. Rep.* 5, 1–10.
602 <https://doi.org/10.1038/srep14340>

603 Song, Y., Cao, C., Qiu, R., Hu, J., Liu, M., Lu, S., Shi, H., Raley-Susman, K.M., He, D., 2019.
604 Uptake and adverse effects of polyethylene terephthalate microplastics fibers on terrestrial
605 snails (*Achatina fulica*) after soil exposure. *Environ. Pollut.* 250, 447–455.
606 <https://doi.org/10.1016/j.envpol.2019.04.066>

607 Sujathan, S., Kniggendorf, A.-K., Kumar, A., Roth, B., Rosenwinkel, K.-H., Nogueira, R., 2017. Heat
608 and Bleach: A Cost-Efficient Method for Extracting Microplastics from Return Activated
609 Sludge. *Arch. Environ. Contam. Toxicol.* 73. <https://doi.org/10.1007/s00244-017-0415-8>

610 Tagg, A.S., Harrison, J.P., Ju-Nam, Y., Sapp, M., Bradley, E.L., Sinclair, C.J., Ojeda, J.J., 2017.
611 Fenton’s reagent for the rapid and efficient isolation of microplastics from wastewater. *Chem*
612 *Commun* 53, 372–375. <https://doi.org/10.1039/C6CC08798A>

613 Talvitie, J., Heinonen, M., Paakkonen, J.-P., Vahtera, E., Mikola, A., Setälä, O., Vahala, R., 2015. Do
614 wastewater treatment plants act as a potential point source of microplastics? Preliminary
615 study in the coastal Gulf of Finland, Baltic Sea. *Water Sci. Technol.* 72, 1495–1504.
616 <https://doi.org/10.2166/wst.2015.360>

617 TextileExchange, 2018. Preferred Fiber & Materials - Market Report 2018.

618 Thiele, C.J., Hudson, M.D., Russell, A.E., 2019. Evaluation of existing methods to extract
619 microplastics from bivalve tissue: Adapted KOH digestion protocol improves filtration at
620 single-digit pore size. *Mar. Pollut. Bull.* 142, 384–393.
621 <https://doi.org/10.1016/j.marpolbul.2019.03.003>

622 Watts, A.J.R., Urbina, M.A., Corr, S., Lewis, C., Galloway, T.S., 2015. Ingestion of Plastic
623 Microfibers by the Crab *Carcinus maenas* and Its Effect on Food Consumption and Energy
624 Balance. *Environ. Sci. Technol.* 49, 14597–14604. <https://doi.org/10.1021/acs.est.5b04026>

625 Welle, F., Franz, R., 2018. Microplastic in bottled natural mineral water—literature review and
626 considerations on exposure and risk assessment. *Food Addit. Contam. - Part Chem. Anal.*
627 *Control Expo. Risk Assess.* 35, 2482–2492. <https://doi.org/10.1080/19440049.2018.1543957>

628 Wypych, G., 2016. *Handbook of Polymers* Ed. 2. Elsevier Science.

629 Zhao, S., Zhu, L., Li, D., 2016. Microscopic anthropogenic litter in terrestrial birds from Shanghai,
630 China: Not only plastics but also natural fibers. *Sci. Total Environ.* 550, 1110–1115.
631 <https://doi.org/10.1016/j.scitotenv.2016.01.112>

632 Zhu, X., Nguyen, B., You, J.B., Karakolis, E., Sinton, D., Rochman, C., 2019. Identification of
633 Microfibers in the Environment Using Multiple Lines of Evidence. *Environ. Sci. Technol.* 53,
634 11877–11887. <https://doi.org/10.1021/acs.est.9b05262>

635 S